

Magnetism near the metal-insulator transition in two-dimensional electron systems: the role of interaction and disorder

S. M. Fazeli and K. Esfarjani

*Department of Physics, Sharif University of Technology,
Tehran 11365-9161, Iran*

B. Tanatar

*Department of Physics, Bilkent University, 06800 Bilkent, Ankara, Turkey
(Dated: October 4, 2018)*

Recent thermodynamic measurements on two-dimensional (2D) electron systems have found diverging behavior in the magnetic susceptibility and appearance of ferromagnetism with decreasing electron density. The critical densities for these phenomena coincide with the metal-insulator transition recorded in transport measurements. Based on density functional calculations within the local spin-density approximation, we have investigated the compressibility and magnetic susceptibility of a 2D electron gas in the presence of remote impurities. A correlation between the minimum in the inverse capacitance ($\partial\mu/\partial n$) and the maximum of magnetization and magnetic susceptibility is found. Based on values we obtain for the inverse participation ratio, this seems to be also the MIT point.

PACS numbers: 71.10.-w, 71.10.Ca, 71.30.+h

Introduction—There has been a large amount of experimental and theoretical activity in recent years to understand the ground state properties of two-dimensional (2D) electron systems¹. Most notably, the observation of a metal-insulator transition (MIT) in these systems provides a major motivation to study the various physical properties. Most experiments perform transport measurements obtaining resistivity or conductivity as a function of temperature at varying electron density to deduce the metallic or insulating phases. In contrast, Ilani *et al.*² used the capacitance technique, a thermodynamic measurement, to measure the compressibility finding that at high densities the results for the inverse capacitance ($\partial\mu/\partial n$) agree with Hartree-Fock or mean-field theories, whereas below the critical density the system becomes very inhomogeneous and $\partial\mu/\partial n$ goes up as the density is lowered. Similar observations were also made by Dultz and Jiang³ on a 2D hole system who noted that the inverse compressibility is minimum at the same density where the MIT occurs.

Recent experiments at in-plane magnetic field concentrated on the spin susceptibility, Lande g -factor, and effective mass of the 2D electron systems present in Si-MOSFETS and GaAs quantum-well structures^{4,5,6,7,8,9}. In particular, Shashkin *et al.*^{10,11} reported a sharp increase of the effective mass near the critical density at which the system starts to show deviations from the metallic behavior. On the other hand, Pudalov *et al.*⁴ have found only moderate enhancement of the spin susceptibility and effective mass in their samples. Thermodynamic measurements of magnetization of a dilute 2D electron system were reported by Prus *et al.*⁸ and Shashkin *et al.*⁹ Both experiments found large enhancement of the spin susceptibility χ_s over its Pauli value. Whereas the measurements of Prus *et al.*⁸ found no in-

dication toward a ferromagnetic instability, Shashkin *et al.*⁹ observed diverging behavior in χ_s at a critical density coinciding with the MIT density obtained from transport measurements.

On the theoretical side, calculation of compressibility for a 2D system of electrons in the presence of disorder predicts the observed behavior of upturn and divergence¹². Shi and Xie¹³ performed density functional calculations based on the (unpolarized) local density approximation developed by Tanatar and Ceperley¹⁴ within the Thomas-Fermi (TF) theory, and found similar results for the compressibility. They also identified the MIT point with the percolation transition point in this system. This theory was further strengthened by Das Sarma *et al.*¹⁵ who measured the critical exponent for the conductivity and found it in agreement with that proposed by percolation theory.

In this work, we investigate the spatial distribution of carrier density and magnetization, as well as the compressibility and spin susceptibility of a 2D electron system using the local spin-density approximation (LSDA) both at the TF and Kohn-Sham (KS) levels. Localization properties are characterized by the inverse participation ratio (IPR). The functional we use is the one constructed by Attacalite *et al.*¹⁶ from the very recent quantum Monte Carlo calculations for correlation energy appropriate for uniform systems. An important feature of these simulations is that a transition to a ferromagnetic phase at low densities is built in the functional. A disorder potential due to remote impurities is included to make the calculation realistic. The density distribution of the system shows high and low density regions as reported earlier by Shi and Xie¹³ which supports the idea of percolation transition. We also find correlated behavior of inverse capacitance minimum and spin susceptibility

maximum, which gives thermodynamic evidence for the appearance of a phase transition. Thus, a unified picture for the thermodynamic behavior of a dilute system of 2D electrons in the presence of disorder emerges from our calculations.

Theory—We consider a 2D electron system interacting via the long range Coulomb interaction $V_q = 2\pi e^2/(\epsilon q)$ where ϵ is the background dielectric constant. The system is characterized by the dimensionless interaction strength $r_s = 1/(\pi n a_B^*)^{1/2}$, where n is the 2D electron density and $a_B^* = \hbar^2 \epsilon / (m^* e^2)$ is the effective Bohr radius defined in terms of the band mass m^* of electrons in the bulk semiconductor structure.

Within the spin-density functional theory the total energy of an N -electron interacting system in a local external potential $V_{\text{ext}}(\mathbf{r})$ is a unique functional of spin-dependent densities $n_\uparrow(\mathbf{r})$ and $n_\downarrow(\mathbf{r})$. The total energy functional can be expressed as

$$E_{\text{Total}}[n_\uparrow, n_\downarrow] = E_T[n_\uparrow, n_\downarrow] + E_H[n_\uparrow, n_\downarrow] + E_x[n_\uparrow, n_\downarrow] + E_c[n_\uparrow, n_\downarrow] + E_{\text{ext}}[n_\uparrow, n_\downarrow].$$

We approximate the kinetic energy functional by the Thomas-Fermi-Weizsäcker (TFW) form given by¹⁷

$$E_T[n_\uparrow, n_\downarrow] = \sum_\sigma \int d\mathbf{r} \left[\pi n_\sigma^2(\mathbf{r}) + \frac{1}{8} \frac{|\nabla n_\sigma(\mathbf{r})|^2}{n_\sigma(\mathbf{r})} \right]. \quad (1)$$

The direct Coulomb energy is given by

$$E_H[n_\uparrow, n_\downarrow] = \frac{e^2}{2} \int d^2\mathbf{r} d^2\mathbf{r}' \frac{n(\mathbf{r}) n(\mathbf{r}')}{|\mathbf{r} - \mathbf{r}'|} \quad (2)$$

where $n(\mathbf{r}) = n_\uparrow(\mathbf{r}) + n_\downarrow(\mathbf{r})$ is the total density. The local spin-density approximation proposed by Attaccalite *et al.*¹⁶ is used to calculate the exchange and correlation potentials.

The disorder studied in this work comes from a random distribution of charged impurities with density n_i and at a setback distance d from the electron layer. The energy functional due to the external potential is

$$E_{\text{ext}}[n] = \int d^2\mathbf{r} V_{\text{ext}}(\mathbf{r}) n(\mathbf{r}) \quad (3)$$

where the external potential, due to remote impurities, is given by

$$V_{\text{ext}}(\mathbf{r}) = - \sum_i \frac{Ze^2/\epsilon}{[(\mathbf{r} - \mathbf{r}_i)^2 + d^2]^{1/2}}. \quad (4)$$

Method—The spin-densities $n_\uparrow(\mathbf{r})$ and $n_\downarrow(\mathbf{r})$ that extremize the total energy functional can be obtained by annealing from a Monte Carlo (MC) simulation. A sufficiently high temperature is first chosen and a Metropolis MC run is performed long enough to reach thermodynamic equilibrium. Then the temperature is reduced and the run is repeated. This is continued until the final temperature is sufficiently low so that very little energy

fluctuations occur during the last run. This simulation is done in order to reach the global minimum of the energy landscape. Once one is near the bottom of the valley, eventually a steepest-descent algorithm is applied to reach the minimum energy structure faster. The areal integral in the energy functional is approximated by a discrete sum: basically the density and potentials are discretized on a 44 by 44 mesh whose size is one effective Bohr radius being equal to 100 Å in GaAs samples. The long-range Coulomb potential is calculated using the Ewald sum method.

The results from the TFW kinetic energy functional were also compared to the solution of the KS equations where the kinetic energy is calculated exactly. We note that a similar Hartree-Fock calculation was recently performed on a Mott insulator in the half-filled limit¹⁸ where the ground state is antiferromagnetic. We believe that the exchange-correlation potential we are using is more realistic, and contains the correct physics, namely that at very low densities, before the Wigner crystallization, the clean system becomes ferromagnetic.

Results and Discussion—For a given distribution of the impurities, the total energy is computed as a function of density. The obtained curve was then fitted with 3 best analytical curves possible and then derivatives were taken analytically in order to reduce fluctuations. The inverse compressibility is obtained as $\kappa^{-1} = n^2 \partial \mu / \partial n$. There is some variations in the results at higher densities, but as Fig. 1 shows, both the minimum and the zeros of $\partial \mu / \partial n$ are identical with reasonably good accuracy.

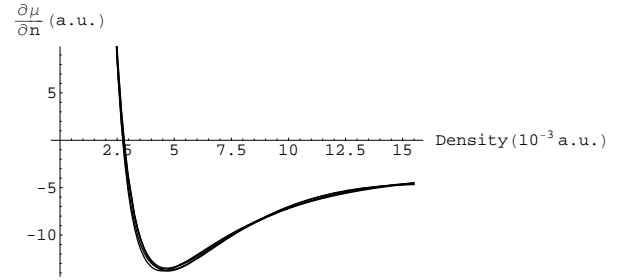


FIG. 1: (Color online) The derivative of the chemical potential versus density, expressed in units of the effective Bohr radius, obtained with the TFW functional. The disorder potential corresponds to a spacer layer of $d = 3$ a.u. and a 2D impurity concentration of $n_i = 2.6 \times 10^{-3}$ a.u. both expressed in units of the effective Bohr radius.

The electron gas was found to have a spin polarization $\xi(r) = [n_\uparrow(r) - n_\downarrow(r)]/n(r)$ reaching a maximum of about 0.05 at $B = 0$ in the low density regions. At lower densities below the minimum in the curve for $\partial \mu / \partial n$ the electron gas separates into electron puddles

where the disorder potential is lowest. Above that critical density there seems to be percolation as noted by Shi and Xie.¹³ The magnetization per electron ($\xi(r)$), as can be observed in Fig. 2, was found to be largest at the critical point (minimum of $\partial\mu/\partial n$) and it was found that both ξ and the susceptibility are highest in the low density regions where the depth of the effective potential ($V_{\text{eff}} = V_{\text{ext}} + V_{\text{Hartree}} + V_{\text{xc}}$) is most shallow.

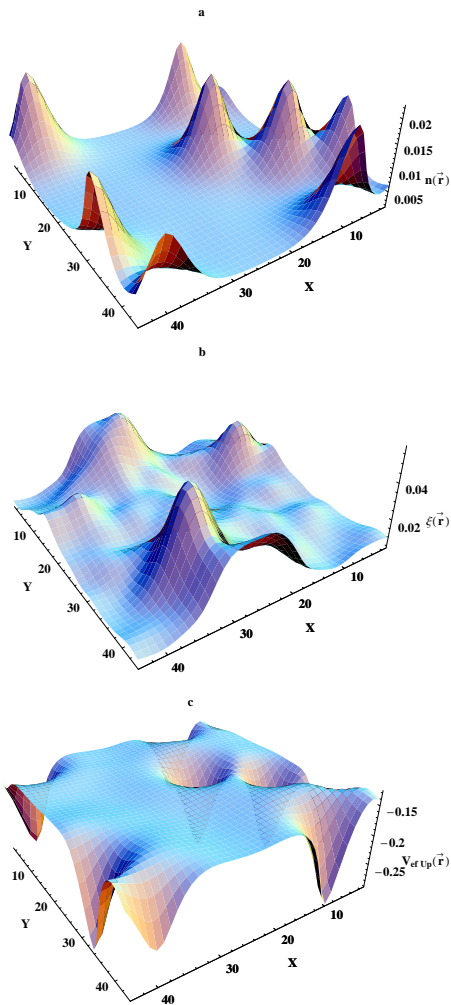


FIG. 2: (Color online) The density, magnetization per particle ξ , and effective potential distribution at the critical point (minimum of $\partial\mu/\partial n$), within the TFW theory. The parameters for this figure are as follows. $d = 3$ a.u., $n_i = 2.6 \times 10^{-3}$ a.u., $r_s = 8$, $n = 5 \times 10^{-3}$ a.u. One can see that the magnetization is largest in the low density or saddle point (for the potential) regions.

To investigate further the effect of the disorder on the spontaneous magnetization of the electron gas, we calculated its magnetic susceptibility by applying an in plane magnetic field to the sample and measure $\chi = M/B_{\parallel}$ at different densities. The effect of the parallel field is only to create a Zeeman splitting in the energy of electrons but the field does not affect their orbital motion as

the system is purely two-dimensional. As can be seen in Fig. 3, even for low fields, both the magnetization and the susceptibility reach their maximum at the density where $\partial\mu/\partial n$ is minimum.

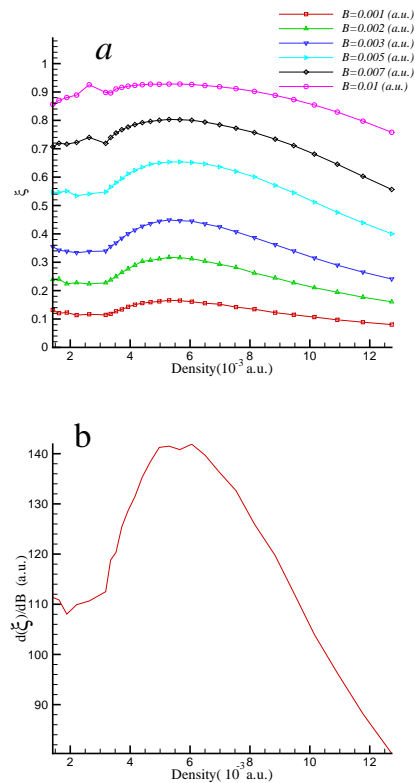


FIG. 3: (Color online) The spin polarization ξ (a) and its derivative χ (b) versus the density for different strengths of the applied parallel field. Impurity parameters are the same as in previous figures. It is seen that the maximum in the magnetization or χ occurs exactly at the density where $\partial\mu/\partial n$ was minimum.

At its minimum, we have $\partial\mu/\partial n < 0$, and according to^{3,13} we are at the percolation transition. An added electron will mostly extend in the percolation region where the density is very low and effective potential flat, and according to our exchange-correlation (XC) functional at low densities, the added electron tends to become magnetized. This tendency is strongest only at the percolation point since at high densities the XC effects do not favor magnetization, and below percolation densities the added electron will tend to be localized in the puddles where again the density is high. To confirm this picture, we need to know the density distribution of the highest occupied and lowest unoccupied states, below and above the Fermi level respectively, where the subtracted or added electrons localize. TFW approximation can not solve for energy levels and eigenstates, but one can extract these levels from the solutions of the KS equations. For the same disorder parameters as above, but for a twice coarser mesh, we have solved the KS equations and

we are displaying in Fig.4 the highest occupied (HOS) and lowest unoccupied (LUS) states at the critical density where $\partial^2\mu/\partial n^2 = 0$.

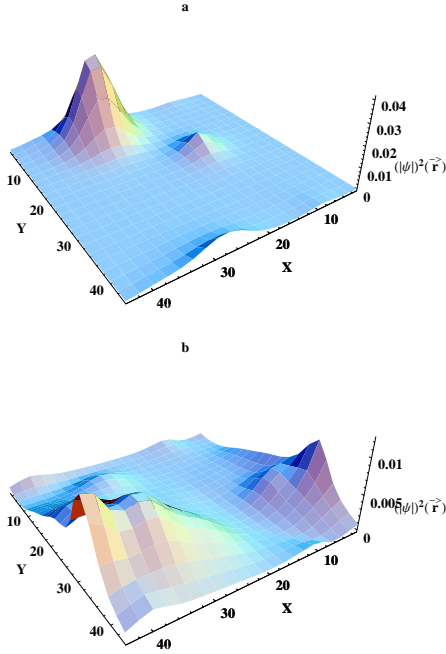


FIG. 4: (Color online) The density distribution of the highest occupied, HOS (a) and lowest unoccupied, LUS (b) states just below and above the Fermi level, respectively, at the critical density where $\partial\mu/\partial n$ is minimum. Fig. 5 shows that they are both down-spin states.

To see whether the HOS and LUS are localized or not, one can compute the inverse participation ratio defined as, $IPR = \int |\psi|^4 d^2r / \int |\psi|^2 d^2r$. For an exponentially localized state in 2D, it gives the square of the inverse localization length. From the KS equations, we have determined the band structure of the finite sample and for the considered system, it turns out that both the HOS and LUS are in the down-spin state, consistent with a large magnetic susceptibility. The IPR is plotted as a function of the energy of the states and displayed in Fig.5. One notices that above the Fermi level, it reaches an almost

constant value of 3, and below this energy it starts going up implying that the HOS seems localized and the LUS is delocalized. This confirms that at the chosen density where $\partial\mu/\partial n$ is minimum, occupied states are localized and unoccupied ones delocalized, meaning that one is also at the MIT point.

Summary—In summary, we have investigated the ground state density and magnetization distribution of an interacting electron system in 2D in the presence of remote impurities. Within the purely thermodynamic calculations based on LSDA, we found that the percolation transition density where the inverse capacitance $\partial\mu/\partial n$ exhibits a minimum, coincides with the MIT based on the IPR results. At the same critical density the mag-

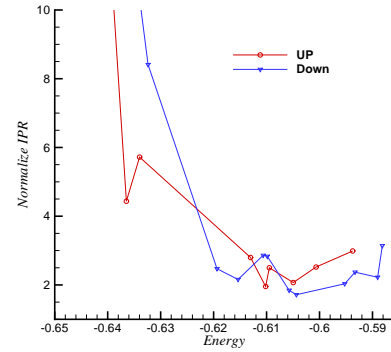


FIG. 5: (Color online) IPR versus the energy in a.u. for the states around the Fermi level (which is at -0.63 a.u.), at the critical density where $\partial\mu/\partial n$ is minimum.

netization and magnetic susceptibility display a maximum where the system goes into a partially polarized ferromagnetic state. and maximum in magnetization are correlated. These calculations suggest that the percolation transition, the ferromagnetic transition and the MIT points are all correlated.

This work is supported by TUBITAK and TUBA. K. E. Would like to thank Prof. A. P. Young and the hospitality of the Physics Department of UC Santa Cruz and Bilkent University where part of this work was performed.

- ¹ E. Abrahams, S. V. Kravchenko, and M. P. Sarachik, Rev. Mod. Phys. **73**, 251 (2001); S. V. Kravchenko and M. P. Sarachik, Rep. Prog. Phys. **67**, 1 (2004).
- ² S. Ilani, A. Yacoby, D. Mahalu, and H. Shtrikman, Phys. Rev. Lett. **84**, 3133 (2000).
- ³ S. C. Dultz and H. W. Jiang, Phys. Rev. Lett. **84**, 4689 (2000).
- ⁴ V. M. Pudalov *et al.* Phys. Rev. Lett. **88**, 196404 (2002).
- ⁵ E. Tutuc, S. Melinte, and M. Shayegan, Phys. Rev. Lett. **88**, 036805 (2002).

- ⁶ J. Zhu, H. L. Stormer, L. N. Pfeiffer, K. W. Baldwin, and K. W. West, Phys. Rev. Lett. **90**, 056805 (2003).
- ⁷ W. Pan, D. C. Tsui, and B. L. Draper, Phys. Rev. B **59**, 10 208 (1999).
- ⁸ O. Prus, Y. Yaish, M. Reznikov, U. Sivan, and V. Pudalov, Phys. Rev. B **67**, 205407 (2003).
- ⁹ A. A. Shashkin *et al.* Phys. Rev. Lett. **96**, 036403 (2006).
- ¹⁰ A. A. Shashkin, S. V. Kravchenko, V. T. Dolgoplov, and T. M. Klapwijk, Phys. Rev. B **66**, 073303 (2002).
- ¹¹ A. A. Shashkin, M. Rahimi, S. Anissimova, S. V.

- Kravchenko, V. T. Dolgoplov, and T. M. Klapwijk, Phys. Rev. Lett. **91**, 046403 (2003); A. A. Shashkin, S. V. Kravchenko, V. T. Dolgoplov, and T. M. Klapwijk, preprint cond-mat/0302004.
- ¹² Q. M. Si and C. M. Varma, Phys. Rev. Lett. **81**, 4951 (1998); R. Asgari and B. Tanatar, Phys. Rev. B **65**, 085311 (2002).
- ¹³ J. Shi and X. C. Xie, Phys. Rev. Lett. **88**, 086401 (2002).
- ¹⁴ B. Tanatar and D. M. Ceperley, Phys. Rev. B **39** 5005 (1989).
- ¹⁵ S. Das Sarma *et al.* Phys. Rev. Lett. **94**, 136401 (2005).
- ¹⁶ C. Attaccalite *et al.* Phys. Rev. Lett. **88**, 256601 (2002).
- ¹⁷ Y. Wang, J. Wang, H. Guo, and E. Zaremba, Phys. Rev. B **52**, 2738 (1995).
- ¹⁸ D. Heidarian and N. Trivedi, Phys. Rev. Lett. **93**, 126401 (2004).